Supporting information for

Asymmetrically Flexoelectric Gating effect of Janus Transition-Metal Dichalcogenides and its Sensor Applications

Kun Peng Dou,[a] Hui Hui Hu,[a] XiaoHan Wang,[a] XinYi Wang,[a] Hao Jin,[*,b] Guang-Ping Zhang,[c] Xing-Qiang Shi[*,d] and Liangzhi Kou[*,e]

[a]College of Information Science and Engineering, Ocean University of China, Qingdao 266100, China

[b]College of Physics and Optoelectronic Engineering, Shenzhen University, Shenzhen 518060, Guangdong, China

[c]Shandong Province Key Laboratory of Medical Physics and Image Processing Technology, School of Physics and Electronics, Shandong Normal University, Jinan 250358, China

[d]College of Physics Science and Technology, Hebei University, Baoding 071002, China

[e]School of Mechanical, Medical and Process Engineering, Queensland University of Technology, Gardens Point Campus, Brisbane, Queensland 4001, Australia

E-mail: jh@szu.edu.cn, shixq@sustech.edu.cn, liangzhi.kou@qut.edu.au

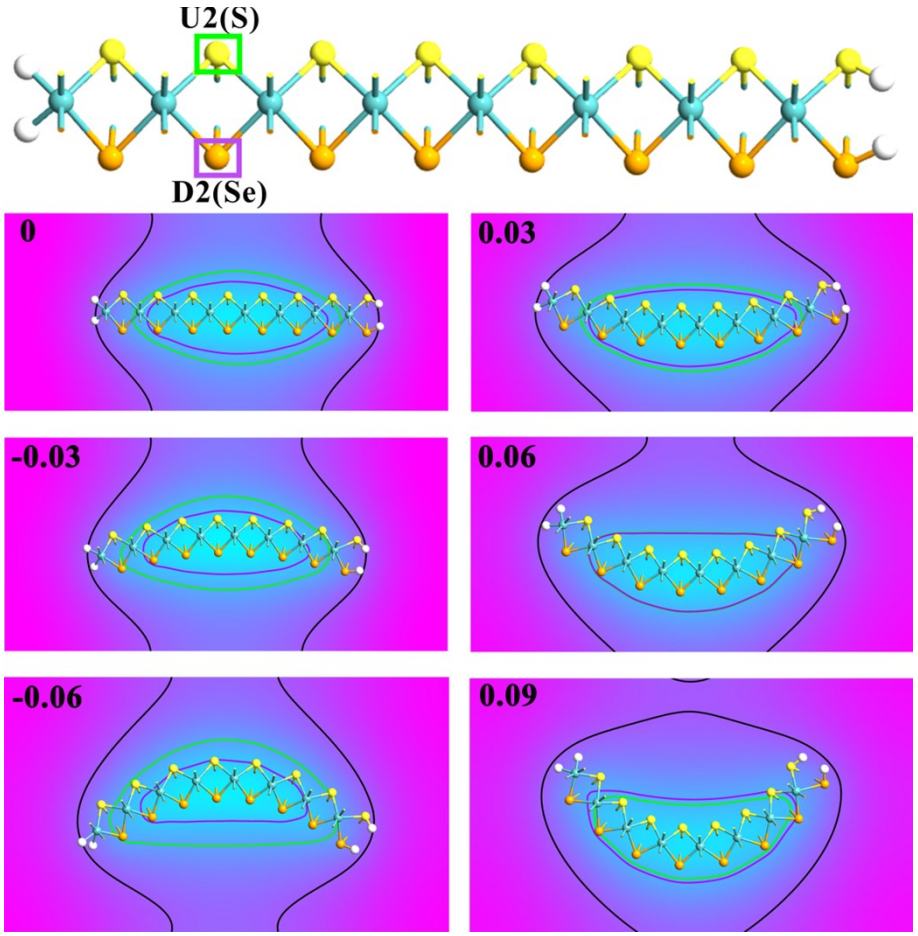

Figure S1 Evolution of the electrostatic potential of armchair MoSeS nanoribbons under several bending curvatures: the isolines cut to Se (D2) and S (U2) are marked by purple and green, respectively. The specific values of the two isolines at each curvature are listed in Table 1, and the black isoline corresponds to 0 Volt. The bending curvatures are labeled and positive/negative value denotes concave/convex bending, respectively.

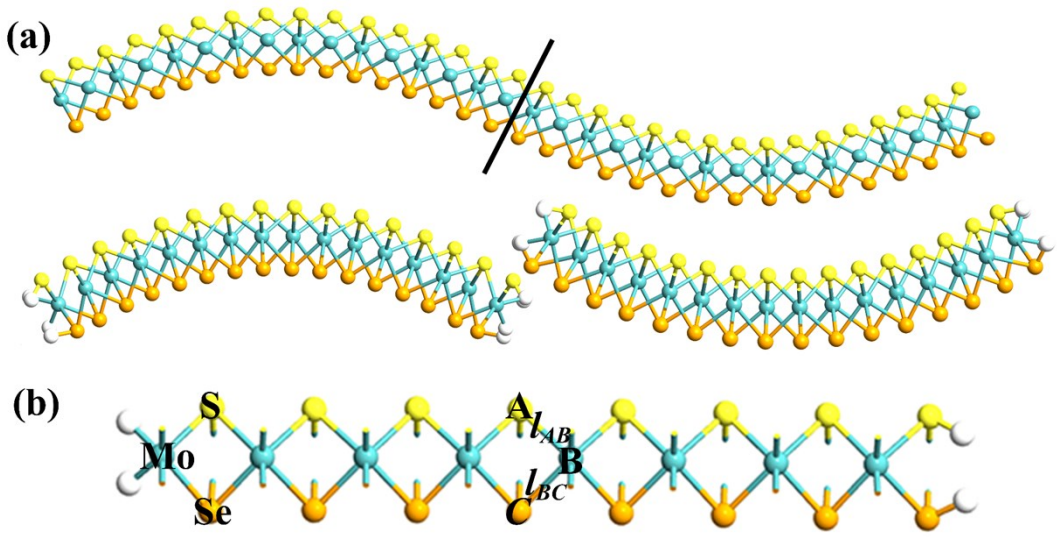

Figure S2. (a) Comparison of ripple and ribbon models for MoSeS, which consisting of thirty-two and sixteen formula units, respectively. (b) Atomic configuration of flat MoSeS ribbon model.

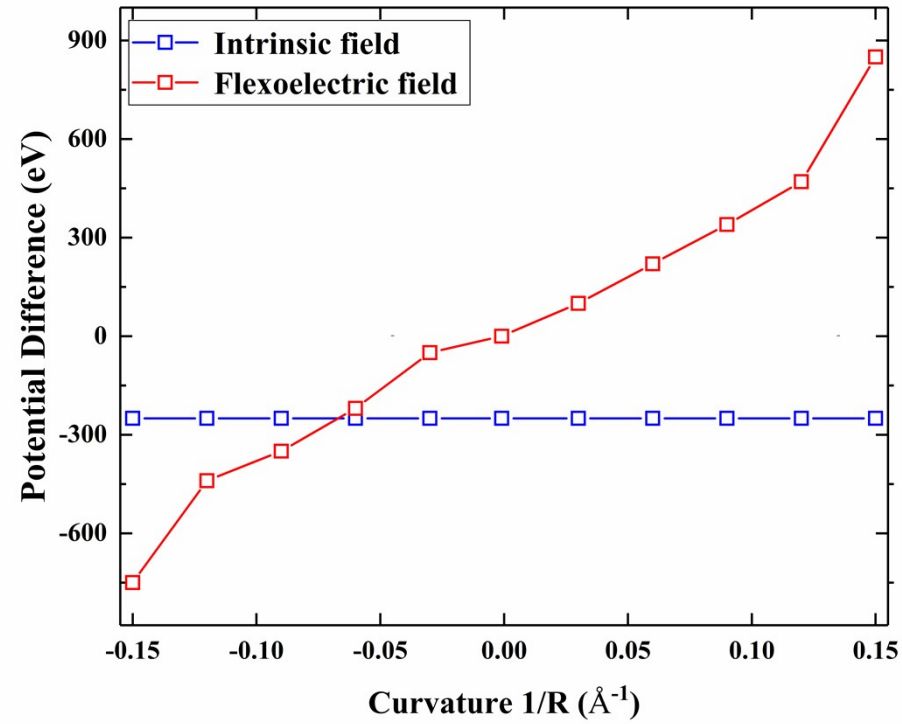

Figure S3. Evolution of intrinsic field and flexoelectric field of MoSeS ribbon model under bending.

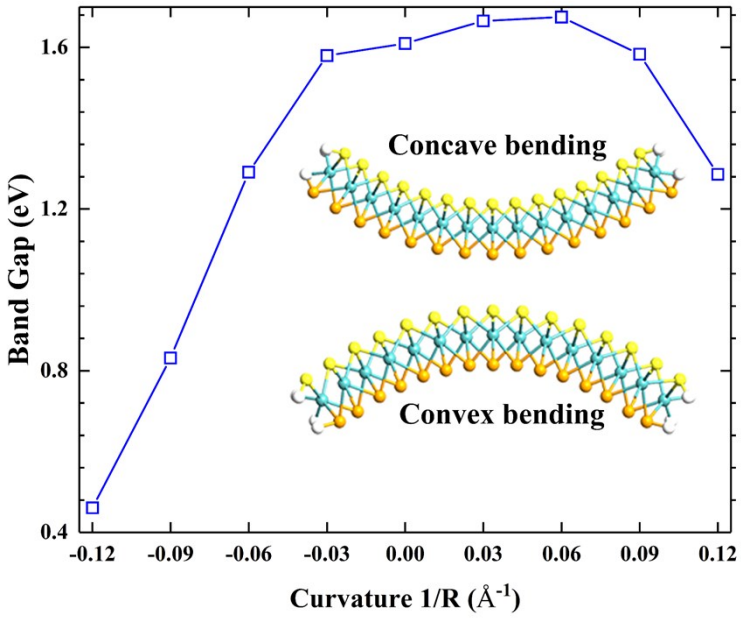

Figure S4. Evolution of bulk band gap of armchair MoSeS nanoribbons with fifteen MoSeS formula units at different curvatures.

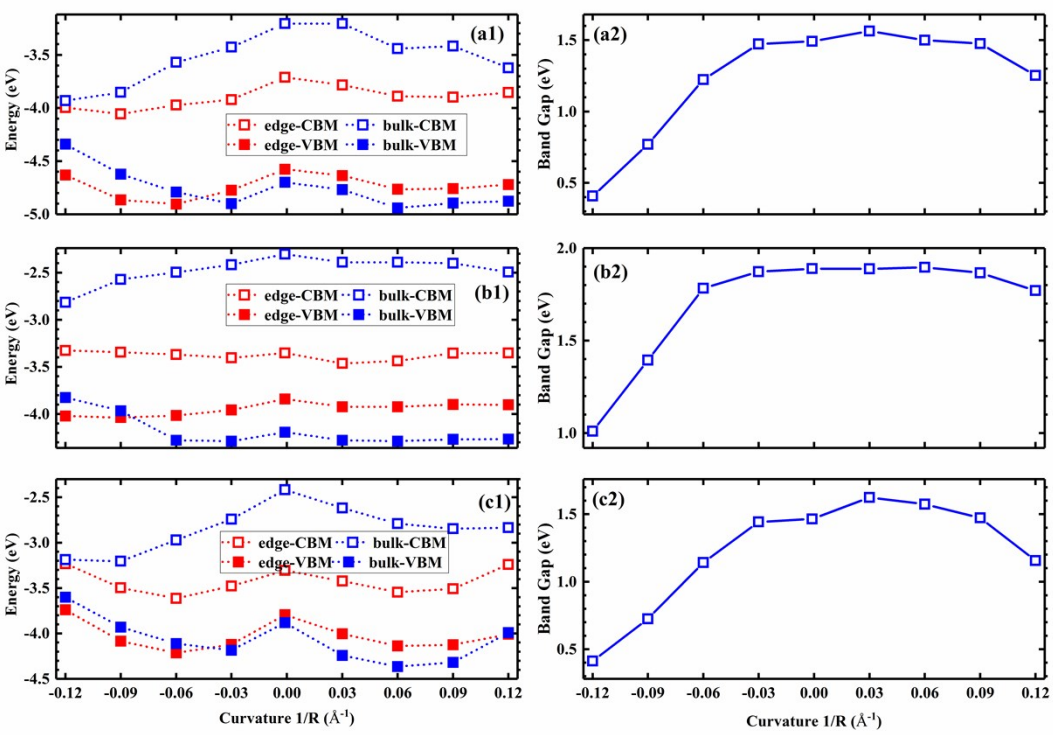

Figure S5 The evolution of band-edge energy-positions and bulk band gap of bending MoSeS nanoribbon under different curvatures: (a1) and (a2) F-terminated armchair MoSeS nanoribbons with sixteen MoSeS formula units; (b1) and (b2) H-terminated armchair MoSeS nanoribbons with eight MoSeS formula units; (c1) and (c2) H-terminated armchair MoSeS nanoribbons with twenty-four MoSeS formula units.

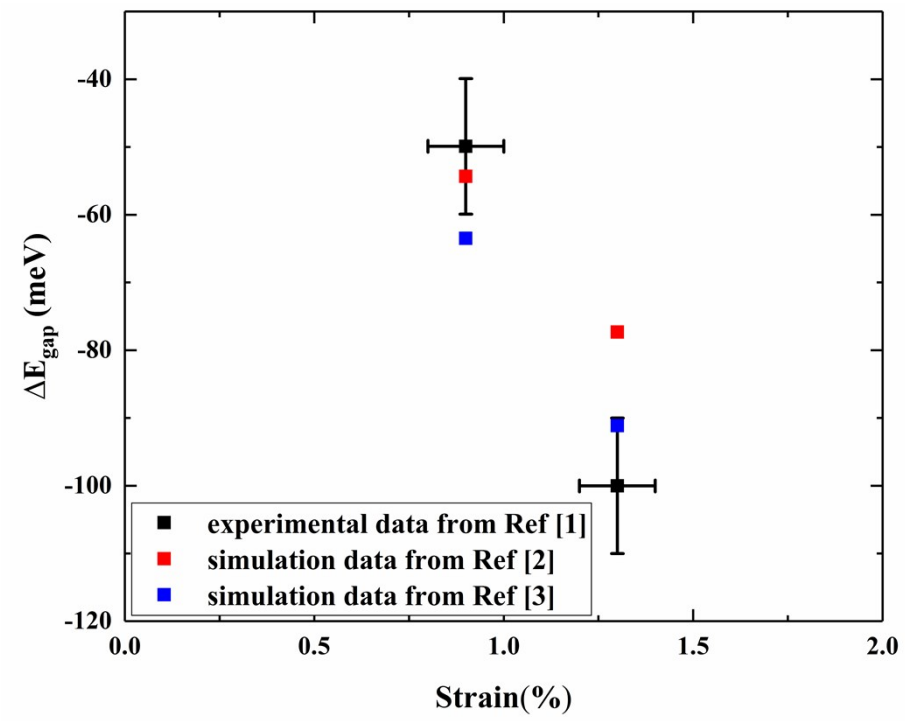

Figure S6 Black points indicate the band gap from experimental work due to uniaxial tensile strain. Error bars are denoted in [Ref. 1], with around ±0.1% in strain determination and an uncertainty of ±10 meV in the extraction of the energy changes. Red and blue data points are the simulated band gap of TMDCs due to uniaxial tensile strain.

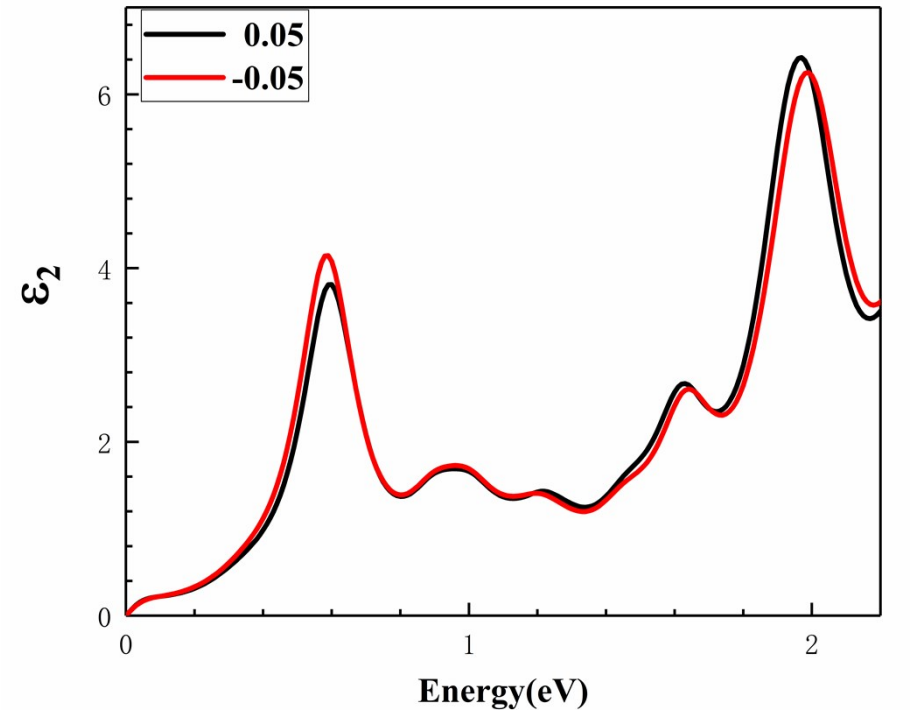

Figure S7. The imaginary part of the dielectric function for MoS_2 under concave/convex bending (0.05 $Å^{-1}$) on dielectric substrate ($4\varepsilon_0$).

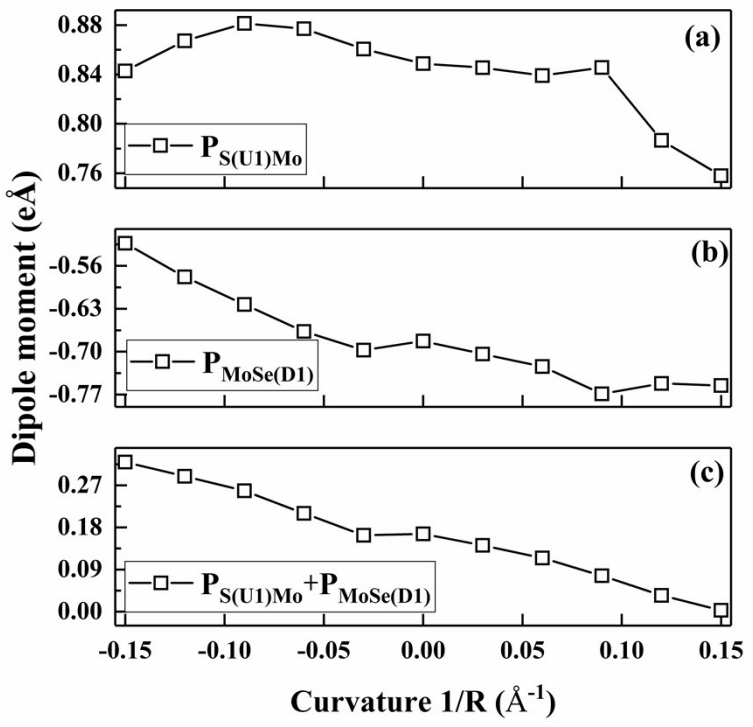

Figure S8. Evolution of dipole moment in the center bulk part of MoSeS ribbon model under bending: (a) dipole moment between atom S_{U1} and its adjacent atom Mo; (b) dipole moment between atom Mo and its adjacent atom Se_{D1}; (c) the total dipole moment across this three atomic layer.

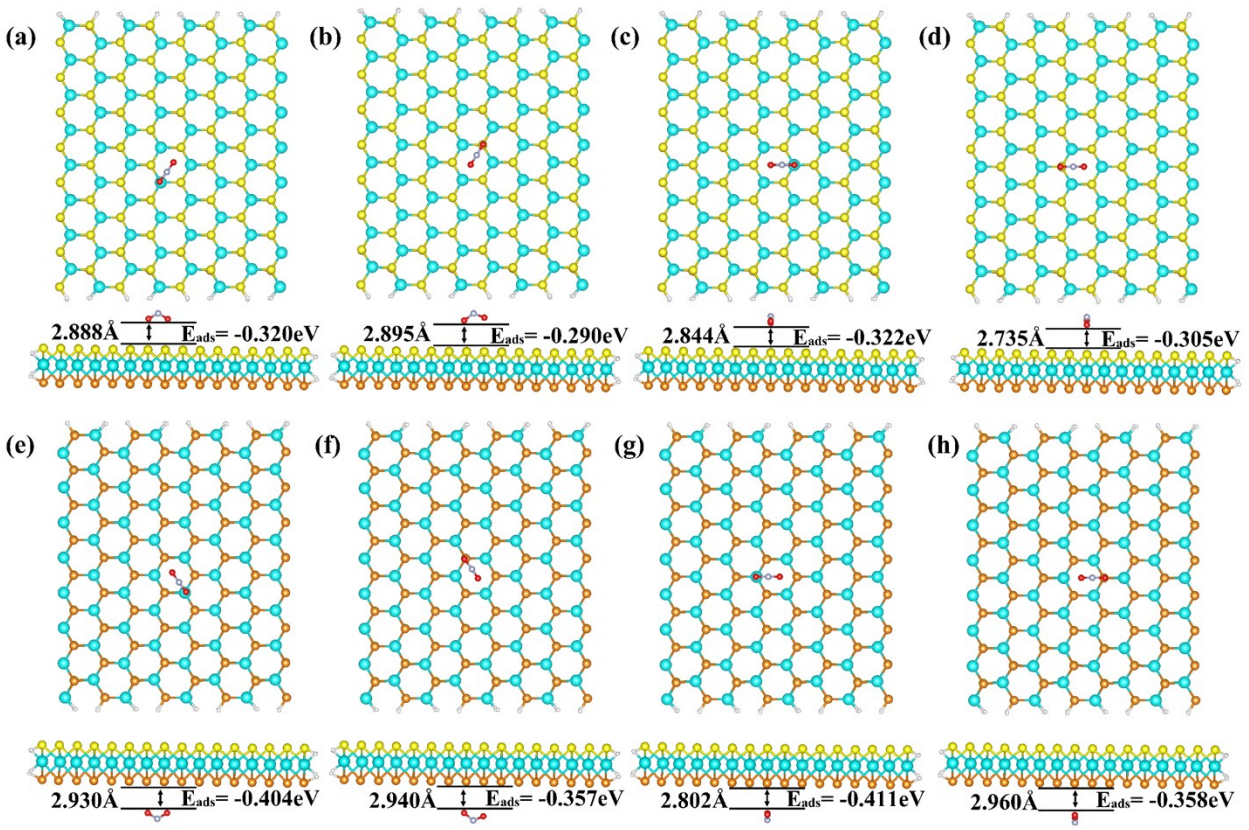

Figure S9. Test calculations to determine the adsorption geometry for NO_2 adsorbed on Se and S layer at 0 $Å^{-1}$. Mo, S and Se atoms are represented by cyan, yellow and orange balls, respectively. The adsorption geometries of (a), (c), (e) and (g) are taken from reference 4. According to the adsorption energy (E_{ads}), the models of (c) and (g) are adopted for the discussion in the context.

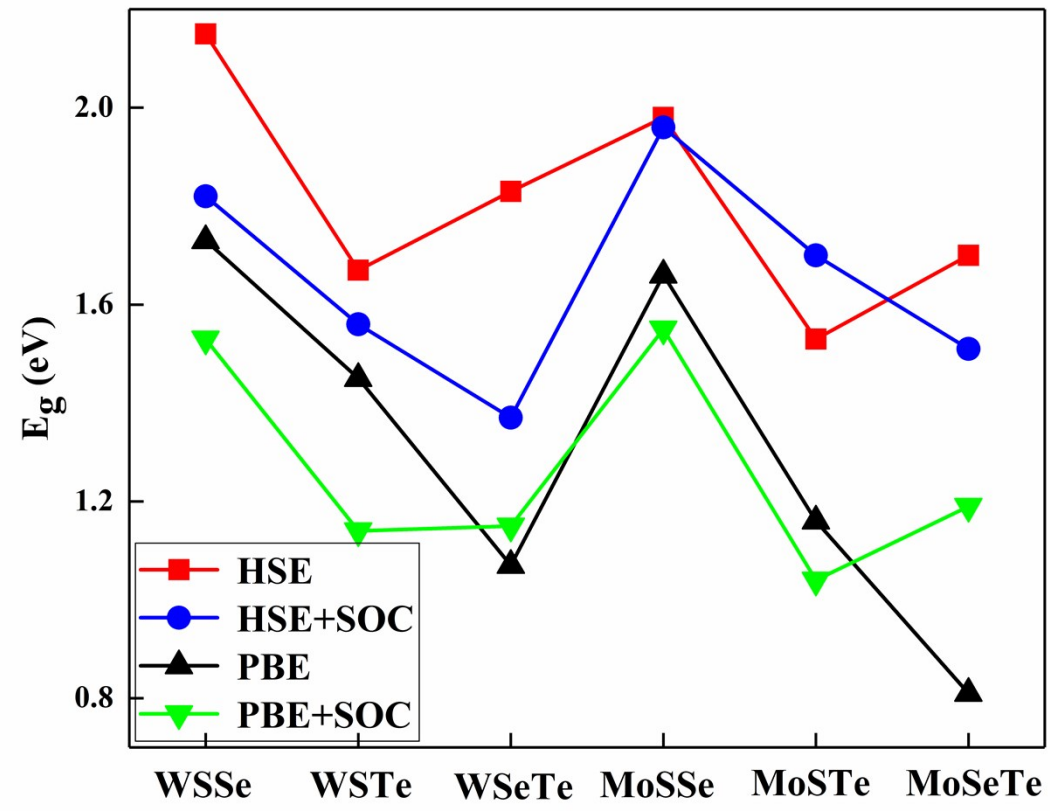

Figure S10. Band gap of Janus monolayer with different calculation sets: (1) gap value by HSE, WSSe (2.15 eV)> MoSSe (1.98 eV)> WSeTe (1.83 eV)> MoSeTe (1.70 eV)> WSTe (1.67 eV)> MoSTe (1.53 eV);[5] (2) gap value by HSE+SOC, MoSSe (1.96 eV)> WSSe (1.82 eV)> MoSTe (1.70 eV)> WSTe (1.56 eV)> MoSeTe (1.51 eV)> WSeTe (1.37 eV);[6] (3) gap value by PBE, WSSe (1.73 eV)> MoSSe (1.66 eV)> MoSTe (1.16 eV)> WSTe (1.45 eV)> WSeTe (1.07 eV)> MoSeTe (0.81 eV);[7] (4) gap value by PBE+SOC, MoSSe (1.55 eV)> WSSe (1.53 eV)> MoSeTe (1.19 eV)> WSeTe (1.15eV)> WSTe (1.14 eV)> MoSTe (1.04 eV).[8]

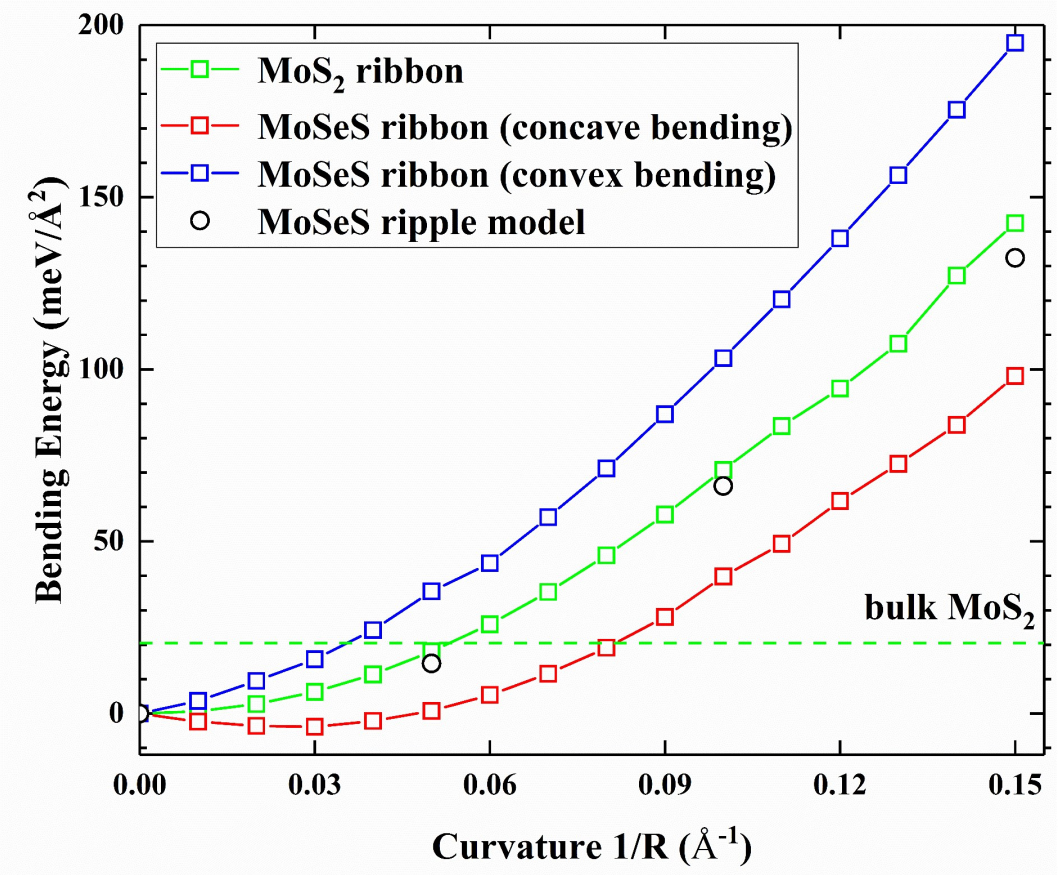

Figure S11. Areal bending energy density. The horizontal dashed line denotes the van der Waals interlayer binding energy of bulk MoS_2.[9] The negative value in concave bending indicates the spontaneous curling in stable freestanding Janus monolayer.[10]

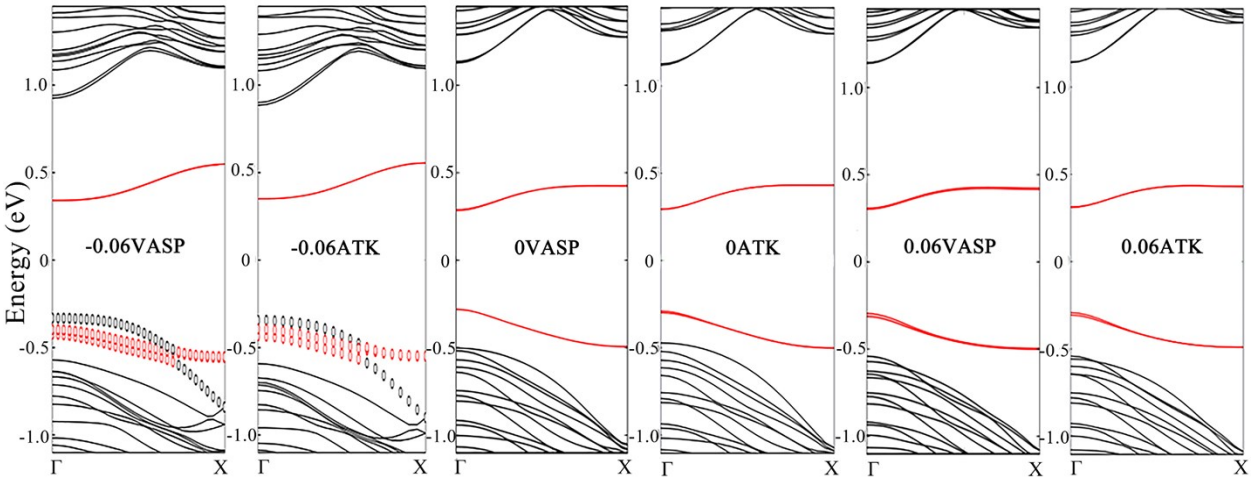

Figure S12 Band structure of armchair MoSeS nanoribbons with sixteen MoSeS formula units at 0 $Å^{-1}$ and ±0.06 $Å^{-1}$ by VASP and QuantumATK.

Table S1. Evolution of electrostatic potential for chosen atoms of armchair MoS_2 nanoribbons under bending. The positions of atoms S (D2), S (D1), S (U2) and S (U1) are the same with those denoted in Figure 2 and Figure S1 for MoSeS.

Curvature ($Å^{-1}$)	$V_{S(D1)}$ (Volt)	$V_{S(U1)}$ (Volt)	$V_{S(D2)}$ (Volt)	$V_{S(U2)}$ (Volt)	$V_{S(D1)}$-$V_{S(U1)}$ (Volt)	$V_{S(D2)}$-$V_{S(U2)}$ (Volt)
0	-1120	-1120	-800	-780	0	-20
0.03	-970	-900	-590	-510	-70	-80
0.06	-1040	-880	-680	-520	-160	-160
0.09	-1080	-830	-720	-540	-250	-180
0.12	-1055	-730	-750	-470	-325	-280
0.15	-1055	-650	-790	-470	-405	-320

Table S2. Evolution of effective mass in bulk conduction band (CB) and valence band (VB) for armchair MoSeS nanoribbons with sixteen MoSeS formula units under bending.

	Curvature ($Å^{-1}$)										
	-0.15	-0.12	-0.09	-0.06	-0.03	0	0.03	0.06	0.09	0.12	0.15
Bulk cb m* (m_0)	0.731	0.755	0.667	0.697	0.631	0.575	0.560	0.557	0.590	0.540	0.459
Bulk vb m* (m_0)	-1.202	-1.671	-2.866	-5.072	-2.721	-2.218	-1.531	-0.811	-3.735	-2.031	-2.981

Table S3. Evolution of ∠ABC and bond lengths l_{BC}, l_{AB} (cf. Figure S2b) for armchair MoSeS nanoribbons with sixteen MoSeS formula units under bending.

	Curvature ($Å^{-1}$)								
	-0.12	-0.09	-0.06	-0.03	0	0.03	0.06	0.09	0.12
∠ABC (°)	74.420	77.500	80.283	81.278	81.096	81.394	81.297	80.278	78.272
l_{AB}	2.545	2.499	2.456	2.430	2.423	2.406	2.390	2.380	2.378
l_{BC}	2.517	2.508	2.507	2.519	2.535	2.546	2.556	2.581	2.612
l_{BC}-l_{AB} (Å)	-0.028	0.009	0.052	0.089	0.112	0.139	0.166	0.201	0.233

Table S4. Evolution of the k-point position which indicates the transition of VBM between bulk state and edge state by convex bending for armchair MoSeS nanoribbon. The term a in "2π/a" is the lattice constant along the periodic direction of this nanoribbon.

Curvature ($Å^{-1}$)	-0.05	-0.06	-0.07	-0.08	-0.09	-0.1	-0.11	-0.12	-0.13	-0.14	-0.15
K ($2\pi/a$)	0.349	0.371	0.407	0.438	0.461	0.475	0.484	0.496	0.499	0.500	0.500

References

1. T. Shen, A. V. Penumatcha and J. Appenzeller, Strain Engineering for Transition Metal Dichalcogenides Based Field Effect Transistors, *ACS Nano*, 2016, **10**, 4712-4718.

2. J. Wiktor and A. Pasquarello, Absolute deformation potentials of two-dimensional materials, *Phys. Rev. B*, 2016, **94**, 245411.

3. P. Johari and V. B. Shenoy, Tuning the Electronic Properties of Semiconducting Transition Metal Dichalcogenides by Applying Mechanical Strains, *ACS Nano*, 2012, **6**, 5449−5456.

4. C. Jin, X. Tang, X. Tan, S. C. Smith, Y. Dai and L. Kou, A Janus MoSSe monolayer: a superior and strain-sensitive gas sensing material, *J. Mater. Chem. A*, 2019, **7**, 1099-1106.

5. H. Liu, Z. Huang, C. He, Y. Wu, L. Xue, C. Tang, X. Qi and J. Zhong, Strain engineering the structures and electronic properties of Janus monolayer transition-metal dichalcogenides, *J. Appl. Phys.*, 2019, **125**, 082516.

6. J. Wang, H. Shu, T. Zhao, P. Liang, N. Wang, D. Cao and X. Chen, Intriguing electronic and optical properties of two-dimensional Janus transition metal dichalcogenides, *Phys. Chem. Chem. Phys.*, 2018, **20**, 18571-18578.

7. D. Er, H. Ye, N. C. Frey, H. Kumar, J. Lou and V. B. Shenoy, Prediction of Enhanced Catalytic Activity for Hydrogen Evolution Reaction in Janus Transition Metal Dichalcogenides, *Nano Lett.*, 2018, **18**, 3943-3949.

8. Y. C. Cheng, Z. Y. Zhu, M. Tahir and U. Schwingenschlögl, Spin-orbit–induced spin splittings in polar transition metal dichalcogenide monolayers, *EPL*, 2013, **102**, 57001.

9. T. Björkman, A. Gulans, A. V. Krasheninnikov and R. M. Nieminen,van der Waals Bonding in Layered Compounds from Advanced Density-Functional First-Principles Calculations, *Phys. Rev. Lett.*, 2012, **108**, 235502.

10. Q. L. Xiong, J. Zhou, J. Zhang, T. Kitamura and Z. H. Li, Spontaneous curling of freestanding Janus monolayer transition-metal dichalcogenides, *Phys. Chem. Chem. Phys.*, 2018, **20**, 20988-20995.